

# Universal Adversarial Perturbation Attacks On Modern Behavior Cloning Policies

Akansha Kalra<sup>\*,1</sup>, Basavasagar Patil<sup>\*,2</sup>, Guanhong Tao<sup>1</sup>, Daniel S. Brown<sup>1</sup>

**Abstract**—Learning from Demonstration (LfD) algorithms have shown promising results in robotic manipulation tasks, but their vulnerability to offline universal perturbation attacks remains underexplored. This paper presents a comprehensive study of adversarial attacks on both classic and recently proposed algorithms, including Behavior Cloning (BC), LSTM-GMM, Implicit Behavior Cloning (IBC), Diffusion Policy (DP), and VectorQuantized-Behavior Transformer (VQ-BET). We study the vulnerability of these methods to universal adversarial perturbations. Our experiments on several simulated robotic manipulation tasks reveal that most of the current methods are highly vulnerable to adversarial perturbations. We also show that these attacks are often transferable across algorithms, architectures, and tasks, raising concerns regarding security vulnerabilities to black-box attacks. To the best of our knowledge, we are the first to present a systematic study of the vulnerabilities of different LfD algorithms to both white-box and black-box attacks. Our findings highlight the vulnerabilities of modern BC algorithms, paving the way for future work in addressing such limitations.

## I. INTRODUCTION

Learning from Demonstration (LfD) has emerged as a powerful paradigm in AI and robotics, enabling agents to acquire complex behaviors from expert demonstrations. These techniques are increasingly deployed in real-world scenarios, such as to enable robots in industrial automation and household robotics. However, these policies pose potential security risks since they can be easily maliciously manipulated by adversaries, causing undesired behaviors or even catastrophic incidents. Motivated by these risks, to the best of our knowledge, we are the first to present a systematic study of the vulnerabilities of a variety of different LfD algorithms to adversarial attacks with a focus on modern behavior cloning algorithms.

Adversarial attacks are a widely studied area in machine learning that aims to develop imperceptible perturbations to change the output of machine learning models. Early work by Szegedy et al. [1] and Goodfellow et al. [2] revealed that adding small, imperceptible perturbations to images could drastically alter the prediction of neural network classifiers. Since then, a significant number of works have explored various attack methods and defense techniques against adversarial attacks [3]–[5].

However, the robustness of LfD models to adversarial attacks has been largely overlooked in prior research, particularly in the context of robotic manipulation tasks. Prior works have only focused on analyzing the vulnerability of a single type of LfD algorithm in isolation [6]–[9]. By

contrast, we perform the first investigation of the relative vulnerabilities of different LfD algorithms under universal adversarial perturbations. In our work we first examine post-deployment white-box attacks, where an adversary has access to the trained model parameters but cannot modify the training process. Unlike training-time attacks that aim to corrupt the learning process, our attacks target the inference phase, attempting to cause task failures through carefully crafted perturbations to visual observations. While prior work focuses on attacks that require expensive test-time optimization of pixel perturbations per input state, we demonstrate the effectiveness of whitebox universal adversarial attacks—attacks that optimize a single perturbation that is designed to work across the entire input distribution—across a variety of LfD algorithms. These attacks are efficient to implement since they do not require any test-time optimization and shed light on the susceptibility of popular LfD algorithms to adversarial attacks. In particular, we evaluate the adversarial robustness of several leading LfD frameworks, including Vanilla Behavior Cloning (BC), LSTM-GMM [10], Implicit Behavior Cloning (IBC) [11], Diffusion Policy [12], and Vector Quantized-Behavior Transformer (VQ-BET) [13] and find that they are all highly susceptible to offline-generated, universal adversarial attacks.

Additionally, while prior work [6]–[9] has only considered white-box attacks, we perform the first analysis of black-box adversarial attacks on LfD policies, where we transfer universal attacks designed for one LfD algorithm to a different algorithm to enable offline-generated, black-box universal adversarial perturbation attacks. In particular, we run black-box transfer attacks to analyze attack transferability across different LfD algorithms, different tasks, and different network architectures. Overall, we hope our results serve as an impetus for enhancing awareness of the security and reliability concerns regarding policies learned via behavior cloning and will inspire researchers to develop more robust LfD algorithms.

The primary contributions of our work are as follows:

- We conduct the first comprehensive study of offline universal adversarial perturbation [14]) attacks across a variety of different behavior-cloning algorithms. In particular, we are the first to study adversarial attacks on LSTM-GMM, IBC, VQ-BET algorithms. We find that all the LfD algorithms studied in this paper are vulnerable to attack.
- We provide the first analysis of black-box transfer attacks on LfD policies and provide insights into the transferability of attacks across algorithms, tasks, and

<sup>\*</sup>Equal Contribution, <sup>1</sup>Kahlert School of Computing, University of Utah, <sup>2</sup>University of California, Irvine

vision backbones. We find surprising transferability of the attacks across all the variations, highlighting the importance of considering robustness in the training pipeline of modern imitation learning.

- We find that, out of all the policies we test, implicit algorithms such as Implicit Behavior Cloning and Diffusion Policy to be the most robust. While recent work [15] has shown that combining a pretrained denoising diffusion probabilistic model and a standard high-accuracy classifier can yield robustness for image classifiers, we are the first to study and showcase the relative robustness of diffusion policies when compared with other LfD approaches.

## II. RELATED WORK

There has been relatively little prior work exploring adversarial attacks on behavior cloning algorithms. Hall et al. [6] provide an early demonstration that vanilla behavior cloning policies can be vulnerable to adversarial perturbations in driving simulations. Wu et al. [7] also explore attacks against a vanilla BC policy trained on image observations. Boloor et al. [8] focus on simple CNN-based BC and demonstrate the vulnerability of end-to-end autonomous driving models to simple physical adversarial examples such as black lines on the road. We note that all three papers only consider online white-box attacks and only attack the steering angle while we attack high-dimensional robot control inputs and consider offline universal attacks in both white-box and black-box settings across multiple LfD algorithms.

Jia et al. [16] show that adversarial patches can directly attack object detectors causing robots to grasp a human hand rather than a card. Unlike our work, which examines the vulnerabilities of modern LfD algorithms, they target traditional object detection models in industrial robots. Other orthogonal work to ours has examined adversarial attacks in human-robot interactions [17], investigated demonstration set poisoning attacks to prevent downstream behavior cloning [18], and has studied language-based universal attacks [19] for language-conditioned policies.

There is also a large body of work on adversarial attacks on RL algorithms [20]–[30]; however, these attacks are specifically designed for reinforcement learning (RL) settings where policies are trained to maximize expected reward, and adversarial perturbations are evaluated or optimized based on their impact on the expected discounted sum of rewards. In contrast, our work is situated entirely in the imitation learning (IL) setting, where no reward signal is available, and policies are learned purely from demonstrations with no access to a simulator for trial and error learning nor for attack generation. As such, the core mechanisms in RL attack methods—including adversarial value estimation, robust policy gradients, and repeated environment interactions for adversarial training—do not apply in our setting.

Prior work by Chen et al. [9], does explore adversarial attacks, but only on diffusion policies [12], while our research examines the vulnerabilities of several different LfD algorithms and also explores how adversarial perturbations

transfer across different algorithms, tasks, and visual backbones, offering a broader and more comprehensive perspective on the vulnerability of modern behavior cloning and the generalizability of such attacks.

In summary, while prior work [6]–[8] demonstrates the vulnerability of individual CNN-based behavior cloning (BC) models in driving domains, our work is the first to systematically study adversarial robustness across a diverse suite of modern imitation learning architectures, including LSTM-GMM, VQ-Transformer, Implicit BC, and Diffusion Policy. In contrast to Chen et al. [9], who focus exclusively on attacking diffusion models, we introduce unified attack methods for a broad range of architectures and evaluate them side-by-side. Finally, our work is the first to study black-box attacks on LfD algorithms via transferability evaluations across algorithms, tasks, and vision backbones, offering insights into shared vulnerabilities that are critical for the design of robust IL systems.

## III. BEHAVIOR CLONING ALGORITHMS

In this section, we provide a brief background and high-level overview of the Behavior Cloning (BC) algorithms we study in this paper. To provide clarity throughout the discussion, we first define some key notations used across these algorithms.

Let  $\Xi$  represent a set of expert trajectory demonstrations, where  $\xi \in \Xi$  is a trajectory consisting of a sequence of state-action pairs  $(s, a)$ , sampled from an expert policy  $\pi^*(s)$ . Our objective in behavior cloning is to learn a policy  $\pi_\theta(s)$ , parameterized by  $\theta$ , that imitates the expert’s behavior by minimizing a loss function  $\mathcal{L}$  that measures the difference between the expert actions and the actions predicted by the learned policy. Formally, for a given policy  $\pi_\theta$ , we aim to minimize:  $\pi_\theta^* = \arg \min_{\pi_\theta} \sum_{\xi \in \Xi} \sum_{s \in \xi} \mathcal{L}(\pi_\theta(s), \pi^*(s))$ , where  $\mathcal{L}$  differs based on the LfD algorithm.

We study 5 different BC approaches in this work. Owing to the space constraints and coupled with the fact these are well-known algorithms, we only describe them briefly here.

**Vanilla Behavior Cloning (BC)** learns a policy via supervised learning [31], [32]. Given a dataset of state-action pairs  $\mathcal{D} = \{(s_t, a_t)\}_{t=1}^N$ , it directly maps states to actions using a neural network,  $\pi_\theta$  trained to minimize the mean squared error (MSE) for continuous actions:

$$\mathcal{L}_{\text{BC}}(\theta) = \frac{1}{N} \sum_{t=1}^N \|\pi_\theta(s_t) - a_t\|_2^2. \quad (1)$$

While effective for simple tasks, Vanilla BC can struggle with tasks requiring long-term dependencies owing to the problem of compounding error and the tasks with multimodality in expert behavior, as it assumes a unimodal distribution over actions [11], [33].

**Long Short-Term Memory with Gaussian Mixture Model (LSTM-GMM)** [10] enhances Vanilla BC by incorporating temporal dependencies through an LSTM network [34]. The LSTM processes a sequence of states  $s_1, s_2, \dots, s_T$  recursively, maintaining an internal hidden state  $h_t$  at each time step. The policy  $\pi_\theta(a_t | s_t, h_{t-1})$  is parameterized by the

LSTM to model the temporal structure and uses a Gaussian mixture model (GMM) [35] to enable multimodal action distributions at each time step:  $p(a_t|s_t, h_{t-1}, \theta) = \text{GMM}(h_t)$ . The policy is trained by maximizing the likelihood of the observed actions given the state sequence:

$$\mathcal{L}_{\text{LSTM}}(\theta) = \sum_{\xi \in \Xi} \sum_{t=1}^T -\log p(a_t|s_t, h_{t-1}, \theta). \quad (2)$$

**Implicit Behavior Cloning (IBC)** reformulates policy learning using energy-based models [11]. Instead of directly predicting actions, IBC learns an energy function  $E_\theta(s, a)$  that assigns low energy to expert actions and high energy to other actions. In IBC, the policy  $\pi_\theta(a|s)$  is learned by optimizing an energy-based model (EBM) that assigns low energy values to actions demonstrated by the expert and higher energy values to other actions. The energy function  $E_\theta(s, a)$  parameterized by  $\theta$  is trained using the InfoNCE loss, for a batch of  $N$  actions:

$$\mathcal{L}_{\text{InfoNCE}}(\theta) = \sum_{i=1}^N -\log \left( \frac{e^{-E_\theta(s_i, a_i)}}{e^{-E_\theta(s_i, a_i)} + \sum_{j=1}^{N_{\text{neg}}} e^{-E_\theta(s_i, \tilde{a}_i^j)}} \right) \quad (3)$$

where  $\tilde{a}_i^j$  for  $j = 1, \dots, N_{\text{neg}}$  are the negative samples and  $i = 1 \dots N$  are the training samples in the batch. The parameters  $\theta$  are optimized by minimizing  $\mathcal{L}_{\text{InfoNCE}}$ , encouraging the model to assign lower energy to expert actions compared to negative samples. This approach allows IBC to capture complex and multimodal action distributions, leading to more robust imitation of expert behaviors [11].

**Diffusion Policy (DP)** [12] models a policy as a conditional denoising diffusion probabilistic model (DDPM) [36] over action sequences. Given a history of states  $S_t = \{s_{t-T_d+1}, \dots, o_t\}$ , the policy defines a conditional distribution  $p_\theta(A_t | O_t)$ , where  $A_t = \{a_t, \dots, a_{t+T_p-1}\}$  is a sequence of future actions. Starting from Gaussian noise  $A_t^K \sim \mathcal{N}(0, I)$ , the policy iteratively denoises via

$$A_t^{k-1} = \alpha_k (A_t^k - \gamma_k \varepsilon_\theta(S_t, A_t^k, k)) + \sigma_k z, \quad z \sim \mathcal{N}(0, I), \quad (4)$$

where  $\varepsilon_\theta$  is a noise-prediction network,  $k = K, \dots, 1$  indexes diffusion steps, and  $\{\alpha_k, \gamma_k, \sigma_k\}$  denote the noise schedule. Training minimizes the mean-squared error between true Gaussian noise  $\varepsilon_k$  and predicted noise  $\varepsilon_\theta$ :

$$\mathcal{L}_{\text{DP}}(\theta) = \mathbb{E}_{A_t, S_t} [\|\varepsilon_k - \varepsilon_\theta(S_t, A_t + \varepsilon_k, k)\|^2]. \quad (5)$$

At inference, the first  $T_a \leq T_p$  actions from the denoised sequence  $A_t^0$  are executed on the robot, and the process is repeated in a receding-horizon manner. This formulation yields stable training, supports multimodal action distributions, and produces temporally consistent action sequences.

**VQ-Behavior Transformer (VQ-BET)** [13] addresses multimodal behavior generation by discretizing continuous robot actions into latent tokens using a Residual Vector Quantization (VQ) module and then modeling these tokens with a GPT-style transformer. This formulation enables VQ-BET to capture diverse behavior modes, handle both condi-

tional and unconditional tasks, and achieve efficient single-pass inference that is faster than diffusion-based policies. Instead of directly predicting high-dimensional continuous actions, VQ-BET first encodes action chunks into a compact latent space, where coarse and fine-grained codes capture multimodal structure. The transformer autoregressively predicts these codes conditioned on past observations (and optional goals), and a lightweight decoder reconstructs actions from the predicted tokens. An additional offset head refines the decoded actions for fidelity. Thus  $\mathcal{L}_{\text{VQ-BET}}$  is defined as:

$$\mathcal{L}_{\text{VQ-BET}}(\theta) = \mathcal{L}_{\text{code}}(\theta) + \left\| A_t - \pi_\theta^{\text{resid}}(S_t) \right\|_1 \quad (6)$$

where  $\mathcal{L}_{\text{code}}$  is a focal loss for predicting the codebook action tokens (see [13] for the full loss formulation). And  $A_t$  and  $\pi_\theta^{\text{resid}}(S_t)$  are ground truth and predicted residual action chunks of size  $n$ , respectively.

#### IV. ADVERSARIAL ATTACK METHODS

In this section we describe our threat model and present a unified framework for performing universal adversarial attacks on different LfD algorithms.

##### A. Threat Model

**Adversary’s Goal:** The attacker aims to cause task failure by perturbing visual observations during deployment, through perturbations that disrupt normal policy execution and cause task failure.

**Adversary’s Knowledge and Capabilities:** Since we study two settings, we first characterize the adversary’s knowledge for white-box attacks and then detail the setting for black-box transfer attacks. **White-Box Attack:** The attacker has white-box access to the trained policy parameters but cannot modify them. Perturbations are limited to the visual observation space (no direct action manipulation). Perturbations must remain within an  $L_p$  norm ball of radius  $\varepsilon$  to maintain imperceptibility. The attacker can compute gradients through the entire policy network. We note that robot state includes eef pose, eef quaternions, and gripper state as input along with the camera images; however, we assume the attacks are only applied to the vision component of the hybrid state. **Black-Box Transfer Attacks:** We study how adversarial perturbations can transfer across different LfD algorithms, model architectures and tasks without requiring access to the target model’s parameters or training data. In these kinds of transfer settings, we assume the attacker seeks to generate effective perturbations using a surrogate model, making these attacks feasible in black-box scenarios. This property significantly broadens the threat surface, as successful attacks can be mounted with minimal knowledge of the target system.

##### B. Universal Adversarial Attacks on LfD Algorithms

We choose a threat model that is particularly relevant for deployed robotic systems using large pre-trained policies, where model weights are publicly available but the training

process is complete. In particular, we study offline Universal Adversarial Perturbations (UAP) that must generate a single fixed perturbation designed to work across all states. The goal of a **Universal Adversarial Perturbations (UAP)** attack [14] is to find a single perturbation vector that can cause misclassification when applied to multiple different inputs. Unlike online attacks such as Fast Gradient Sign Method (FGSM) [2] or Projected Gradient Descent (PGD) [37] attacks, which compute perturbations for each input independently and require expensive white-box access at test-time, UAP generates a single perturbation  $v$  that satisfies  $\|v\|_p \leq \epsilon$  and is designed offline to successfully affect a high fraction of the input distribution. The perturbation is computed iteratively over a set of training inputs by accumulating the minimal perturbation needed to cause misclassification for each input while maintaining the constraint on the perturbation magnitude.

We formulate the universal perturbation search as the following maximization problem:

$$\max_{\|\delta\|_\infty \leq \epsilon} \mathbb{E}_{(s,a) \sim \mathcal{D}} \left[ -\mathcal{L}(\pi_\theta(s + \delta), a) \right], \quad (7)$$

where  $\pi_\theta$  is the behavior cloning,  $s$  are image observations,  $a$  are ground-truth actions, and  $\mathcal{L}$  is the loss computed according to choice of underlying behavior cloning. This approach is particularly relevant for real-world scenarios where computing per-input perturbations may not be feasible, and the same attack vector needs to work across multiple observations.

---

**Algorithm 1** Universal Adversarial Perturbation Attack for BC Policy

---

**Require:** Dataset  $\mathcal{D}$  of trajectories states  $s$  and actions  $a$ , BC policy  $\pi_\theta$ , perturbation budget  $\epsilon$ , step size  $\alpha$ , epochs  $E$

- 1: Initialize universal perturbation  $\delta = 0$
- 2: **for** epoch  $e = 1$  to  $E$  **do**
- 3:     Reset gradient accumulator  $G = 0$
- 4:     **for** each batch  $(s, a)$  from  $\mathcal{D}$  **do**
- 5:         Form perturbed input  $\tilde{s} = \text{clip}(s + \delta, 0, 1)$
- 6:         Predict actions  $\hat{a} = \pi_\theta(\tilde{s})$
- 7:         Compute  $\mathcal{L}(\hat{a}, a)$  according to chosen BC policy
- 8:         Accumulate input sensitivity:  $G += \nabla_{\tilde{s}} \mathcal{L}$
- 9:     **end for**
- 10:     Update perturbation:  $\delta \leftarrow \text{clip}_{[-\epsilon, \epsilon]}(\delta + \alpha \cdot \text{sign}(G))$
- 11: **end for**
- 12: **return**  $\delta$

---

Algorithm 1 presents a unified UAP attack framework that applies to all BC models considered in this paper. Given a dataset  $\mathcal{D}(s, a)$  of state-action pairs, a perturbation budget  $\epsilon$ , step size  $\alpha$ , and epochs  $E$ , we optimize a single universal perturbation  $\delta$  that maximizes the policy-specific training loss. At each epoch, perturbed states  $\tilde{s} = \text{clip}(s + \delta, 0, 1)$  are passed through  $\pi_\theta$ , gradients of the relevant loss function are accumulated, and  $\delta$  is updated under the  $\ell_\infty$  constraint  $|\delta|_\infty \leq \epsilon$ .

For Vanilla BC, the adversarial attacks aim to maximize the mean squared error (MSE) loss (Equation (1)) between

the predicted and expert actions by introducing small perturbations to the input states. In LSTM-GMM, the attacks target the temporal dependencies modeled by the LSTM and the multimodal action distributions captured by the Gaussian Mixture Model (GMM), aiming to disrupt the likelihood maximization over the GMM outputs (Equation (2)).

Implicit BC algorithms differ from explicit ones in modeling the learning process and action selection. For the attack on IBC, the objective is to perturb the state  $s$  by finding a perturbation  $\delta$  that increases the energy (reduces the probability) of the correct action at that state (Equation (3)). To formulate a universal adversarial attack for Diffusion Policy (DP) we use the MSE loss between the predicted “denoised” actions on the perturbed observation with the random noise added and the actual added noise perturbation. (Equation (5)). Finally, for VQ-BET, the attacks exploit the latent action space by targeting the prediction loss of discrete latent codes (Equation 6), ultimately leading to suboptimal action predictions.

## V. EXPERIMENTS & RESULTS

We design our experiments to answer the following questions: (1) How vulnerable are different modern behavior cloning algorithms to adversarial attacks? (2) How sensitive are attacks to the range of adversarial perturbation? (3) How transferable are the attacks across different algorithms and different tasks? (4) What is the impact of different feature extraction backbones on attack performance, as in how transferable are the attacks between different vision architectures?

### A. Environments

To demonstrate the adversarial robustness of modern behavior cloning algorithms, we consider a set of common benchmarks shown in Figure 1. The tasks of Lift, Can and Square are taken from Robomimic [10], where the state-of-the-art frameworks such as Diffusion Policy and LSTM-GMM have been shown to have a nearly 100% success rate in non-adversarial settings. All 3 tasks Lift, Can and Square have a 7d action space with 84x84 image observations. We also consider the Push-T environment, first introduced by [11] and then subsequently used by Diffusion Policy [12] and VQ-BET [13].

**Lift** is a simple task where a robot arm must lift a small cube from a table surface. The task tests basic pick-and-place capabilities and serves as an entry-level benchmark. Success is determined by elevating the cube above a threshold height. Initial cube poses are randomized with z-axis rotation within a small square region at the table center. **Can** requires the robot to transfer a soda can from a large source bin into a smaller target bin. This task presents increased difficulty over Lift due to the more complex grasping requirements of the cylindrical can and the constrained placement target. The can’s initial pose is randomized with z-axis rotation anywhere within the source bin. **Square** is a high-precision manipulation task where the robot must pick up a square nut and insert it onto a vertical rod. This task significantly

BC Policy \ Task	Lift		Push-T		Can		Square	
	Unattacked	Attacked	Unattacked	Attacked	Unattacked	Attacked	Unattacked	Attacked
Vanilla BC	0.94 (0.02)	0.00 (0.00)	0.65 (0.05)	0.10 (0.00)	0.80 (0.10)	0.00 (0.00)	0.20 (0.06)	0.00 (0.00)
LSTM-GMM	0.98 (0.00)	0.00 (0.00)	0.69 (0.04)	0.09 (0.02)	0.10 (0.00)	0.00 (0.00)	0.82 (0.08)	0.00 (0.00)
IBC	0.77 (0.12)	0.71 (0.08)	0.72 (0.01)	0.57 (0.05)	0.07 (0.02)	0.00 (0.00)	0.03 (0.03)	0.00 (0.00)
DP	1.00 (0.00)	0.00 (0.00)	0.89 (0.00)	0.25 (0.05)	1.00 (0.00)	0.00 (0.02)	0.99 (0.03)	0.00 (0.00)
VQ-BET	1.00 (0.00)	0.00 (0.00)	0.62 (0.03)	0.08 (0.00)	0.96 (0.03)	0.00 (0.00)	0.59 (0.05)	0.00 (0.00)

TABLE I: **Robustness of BC policies to UAP attacks:** Task success rates (Mean  $\pm$  Std) under unattacked and UAP attack for BC, LSTM-GMM, IBC, DP, and VQ-BET across all 4 tasks starting from left to right: Lift, Push-T, Can, and Square task. Our results demonstrate that explicit BC methods (Vanilla BC, LSTM-GMM and VQ-BET) are highly vulnerable, while implicit methods (IBC and DP) maintain comparatively higher success on some of the simpler tasks, but are still highly vulnerable, especially for more complex tasks like Can and Square.

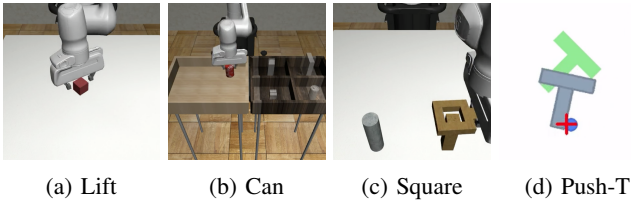


Fig. 1: **Environments used** : for crafting and evaluating Universal Adversarial Perturbation attacks to study adversarial robustness of modern behavior cloning algorithms. (a)-(c) are from RoboMimic [10] and (d) is from [11].

increases complexity by requiring precise alignment and complex insertion dynamics. The nut’s initial pose is randomized with z-axis rotation within a square region on the table surface. **Push-T** is a contact-rich manipulation task where the robot must guide a T-shaped block to a fixed target location using a circular end-effector. We use the vision-variant of Push-T with 2-dim action space and  $3 \times 96 \times 96$  image observation. The task requires precise control of contact dynamics, as the robot must strategically apply point contacts to maneuver the block along the desired trajectory. Unlike pick-and-place tasks, success depends on understanding and exploiting the complex dynamics of planar pushing. We evaluate using RGB image observations augmented with end-effector proprioception. Initial positions of both the T-shaped block and the end-effector are randomized to ensure learned policies must generalize across different pushing strategies.

### B. Pretrained Policies

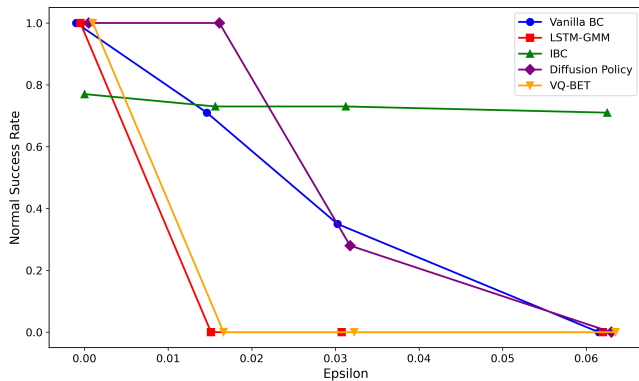
To provide consistent and reproducible results, we attack the pre-trained checkpoints for LSTM-GMM, IBC, and DP released by the authors of Diffusion Policy [12] on these suite of tasks, and train our policies for Vanilla-BC and VQ-BET, due to absence of publicly available checkpoints. Note we use CNN variant of diffusion policy. We evaluate all the environments on 50 randomly initialized environments across 3 different seeds for reporting the mean and standard deviation of the success rate. For our attacks on Lift, Can, and Square we use the proficient human demonstration datasets from Robomimic [10] and attack both camera views: front-view camera and the wrist-mounted camera. For the adver-

serial attacks we use an overall attack budget of  $\epsilon = 0.0625$  (16/256) and clamp the universal perturbation generated to be in  $[-\epsilon, \epsilon]$  range. We also clip the perturbed observations (observations with universal perturbations added) to be in  $[0, 1]$  range. The source code including the checkpoints for this project will be released publicly at [link to be inserted after review].

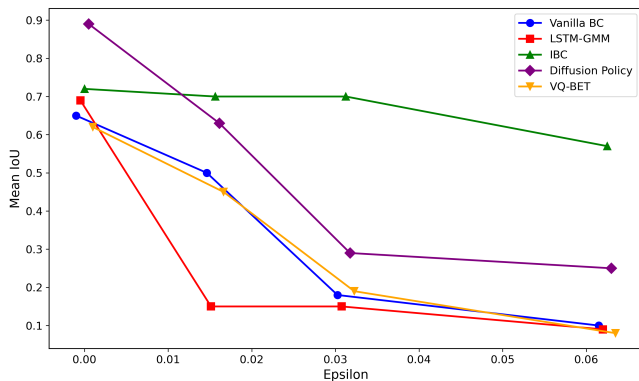
### C. How vulnerable are different modern behavior cloning algorithms to adversarial attacks?

To assess the vulnerability of modern behavior cloning algorithms to adversarial attacks, we conducted a comprehensive evaluation using offline (UAP) attack methods.

Our findings, as illustrated in Table I reveal significant vulnerabilities in the adversarial robustness of current algorithms when faced with perturbations in the observation space. Explicit BC algorithms are very susceptible to UAP attacks. This is evidenced by Task Success Rate in Lift (first column in Table I, dropping from unattacked 0.94 to only 0 under UAP attack for BC, We observe a similar trend across Push-T, Can, and Square as well. In contrast, algorithms employing iterative methods for action selection, such as IBC, exhibited relatively higher robustness in both Lift and Push-T, while DP displayed a high robustness to UAP attack in Push-T where its Task Success Rate drops from 0.89 when unattacked to 0.25 when attacked. We conjecture that this enhanced resilience of implicit algorithms can be attributed to the inherent stochasticity in their action selection processes during inference. It is important to note that the effectiveness of these attacks varies depending on the complexity of the task environment. For instance, the Lift environment allows for a larger margin of error, making it more forgiving to substantial perturbations in actions. However, as task complexity increases, we observe a dramatic reduction in the robot task success rates (increase in attack success rates) across all algorithms. Mandelkar et al. [10] categorized the difficulty of the tasks with *Lift* being the easiest, *Can* being harder than *Lift*, and *Square* being harder than *Can*. As we increase the complexity of the task, we notice an increase in the efficacy of the adversarial attacks.



(a) Lift



(b) Push-T

Fig. 2: **Task Success Rates under decreasing attack strength** ( $\epsilon$ ) of different behavior cloning algorithms demonstrating their sensitivity to even small adversarial inputs. The steep drop in performance of all BC algorithms except IBC, which suffers a minimal drop, emphasizes the lack of robustness across algorithms.

#### D. How sensitive are attacks to the range of adversarial perturbation?

We systematically vary attack strength  $\epsilon$  to determine if our results from Table I depicting susceptibility of BC algorithms still hold with weaker attacks.

Our analysis in Figure 2 reveal that vulnerabilities in behavior cloning algorithms exist even with minimal perturbations in our UAP attacks. We observe in Figure 2 that while decreasing epsilon values generally reduces attack efficacy, as expected, algorithms like Vanilla BC, VQ-BET, LSTM-GMM, and Diffusion Policy still exhibit substantial performance degradation even at very small epsilon values ( $\epsilon$  of  $4/256$  which is approximately 1.5% of the input range). This heightened sensitivity to small perturbations highlights a concerning vulnerability in current behavior cloning approaches, suggesting that even well-constrained adversarial attacks can significantly compromise policy performance.

Interestingly, we find that implicit policies are significantly more robust to adversarial perturbations than explicit policies under white-box UAP attacks. Among implicit methods, IBC displays the highest robustness, surpassing Diffusion Policy. We believe that this stems from IBC’s contrastive sampling,

which provides redundancy against fixed perturbations while Diffusion Policy employs a stochastic multi-step denoising process in which the fixed UAP perturbation is propagated through the entire denoising chain in a coherent way, leading to a more consistent shift in the resulting action sequence. These differences suggest that each model’s inference dynamics play a central role in shaping its vulnerability, and future work could explore this further via step-wise attack tracing or ablations over the inference pipeline.

#### E. Can adversarial examples transfer across different algorithms and tasks?

The transferability of adversarial examples across different behavior cloning algorithms presents an intriguing phenomenon to study, especially given the substantial differences in their loss functions and training methodologies (as detailed in Section III). While these algorithms share a common image encoder (ResNet-18), their end-to-end training approaches may result in distinct feature representations. We conduct black-box transferability attacks to investigate (1) whether the UAP attack crafted for one LfD algorithm generalizes to other algorithms within the same task, and (2) whether the UAP attack generated for a task can transfer to unseen tasks when the LfD algorithm is held fixed.

From Table II, we observe that in simpler environments like the Lift task, where baseline success rates are high ( $>90\%$  for most algorithms), we observed limited transferability with relatively small proportional drops in performance, aligning with our initial expectations. While, interestingly, in the Push-T environment we noticed high-transferability of attacks between algorithms except for Diffusion Policy. As we progressed to more complex environments such as Can and Square, in which the baseline success rates are itself lower and the tasks are naturally less robust to action perturbations, we noticed that transferred attacks often caused larger proportional drops in performance relative to the baseline. For instance, Row 2 of Table II shows that a UAP crafted using BC reduces IBC’s task success rate to 0.8 in Column *Lift*, 0.41 in *Push-T*, and completely to 0 in for tasks *Can* and *Square*.

Now that we have seen black-box transferability of UAP attacks across algorithms, we summarize our results of investigating question (2) about inter-task transfer in Table III. Our results in Table III, where we report the percentage decrease in the robot task completion rate compared to the non-attacked version, show that the attacks developed in Lift can transfer to both the other environments (Can and Square). Because Vanilla BC and IBC struggle to learn a good policy for Square and IBC fails to learn a good policy for Can, we focus our analysis on LSTM-GMM, DP, and VQ-BET. While UAPs generated on Lift reduce Can task performance by  $\geq 40\%$  across LSTM-GMM, DP, and VQ-BET, they also cause a measurable drop in Square performance, despite weaker transferability. This cross-task vulnerability of UAP attacks, highlights the limited robustness of current behavior cloning methods.

Attacker \ Target Policy	Lift					Can					Square					Push-T				
	BC	LSTM	IBC	DP	VQ	BC	LSTM	IBC	DP	VQ	BC	LSTM	IBC	DP	VQ	BC	LSTM	IBC	DP	VQ
Random	0.96	0.84	0.80	1.00	0.98	0.62	0.94	0.00	1.00	0.96	0.42	0.36	0.00	0.98	0.64	0.60	0.61	0.64	0.82	0.55
Vanilla BC	0.00	0.00	0.80	1.00	0.94	0.00	0.66	0.00	0.42	0.88	0.00	0.08	0.00	0.94	0.38	0.10	0.08	0.41	0.80	0.22
LSTM-GMM	0.94	0.00	0.72	1.00	0.96	0.18	0.00	0.00	0.72	0.68	0.18	0.00	0.00	0.96	0.62	0.15	0.09	0.33	0.78	0.31
IBC	1.00	0.10	0.64	1.00	0.98	0.72	0.98	0.00	1.00	0.92	0.42	0.10	0.00	0.98	0.62	0.14	0.08	0.14	0.71	0.17
DP	0.82	0.22	0.78	0.00	0.94	0.02	0.24	0.00	0.00	0.70	0.00	0.00	0.00	0.32	0.27	0.10	0.24	0.14	0.22	
VQ-BET	0.94	0.50	0.84	1.00	0.00	0.34	0.64	0.00	0.42	0.04	0.26	0.00	0.00	0.98	0.00	0.26	0.14	0.47	0.61	0.08

TABLE II: **Inter-Algorithm Black-Box Transferability of UAP attacks on Lift, Can, Square and Push-T**: Each row shows perturbations crafted by the attacker algorithm, applied to target policies in columns under the same task. Each cell represents average success rates of target policies under UAPs generated from different attacker policies within same task. Diagonal entries quantify within-algorithm vulnerability, while off-diagonal entries measure cross-algorithm transferability. To save space, we abbreviated the names of the different LfD algorithms across the second row.

Attacker \ Target Policy	Lift	Can	Lift-to-Can	Square	Lift-to-Square
LSTM-GMM	100%	100%	40%	100%	38.9%
DP	100%	100%	45%	100%	6.6%
VQ-BET	100%	100%	0%	100%	11.4%

TABLE III: **Inter-Task Black Box Transferability of UAP attacks**: Percentage decrease in task completion rate (i.e., success rate reduction) when UAP attacks generated in Lift task are applied to other tasks (Can, Square) holding the BC algorithm constant.

#### F. What is the impact of different feature extraction backbones to attack performance?

To further investigate the black-box transferability across vision backbones, we crafted UAP attacks on BC policies trained with ResNet-18 and directly applied these attacks to ResNet-50-based BC policies. Table IV reveals substantial cross-backbone transferability for Vanilla-BC, LSTM-GMM and IBC in the Lift task, whereas Diffusion Policy and VQ-BET exhibit higher robustness.

Table V and Table VI shows that in the more challenging tasks (Push-T and Can), all algorithms with ResNet-50 backbone are highly vulnerable to black-box transferred UAP attack crafted with ResNet-18 vision backbone. These results demonstrate that ResNet-50 models are still susceptible to ResNet-18-crafted perturbations, indicating that backbone size alone does not mitigate vulnerabilities. Our results underscore the importance of considering cross-architecture vulnerabilities in the design of robust behavior cloning systems.

## VI. CONCLUSION & FUTURE WORK

Our results show that modern behavior cloning algorithms are vulnerable to adversarial attacks. Interestingly, implicit policies such as Implicit Behavior Cloning and Diffusion Policy seem to be more robust than the explicit policies. However, our results also demonstrate that the attack success rate is dependent on the task. As tasks gets harder, it becomes easier to attack these algorithms.

This also holds true based on the results from transferability of attacks between different algorithms. We also show

Algorithm \ Backbone	ResNet-18		ResNet-50	
	Unattacked	Attacked	Unattacked	Attacked
Vanilla BC	1.00	0.21	1.00	0.75
LSTM-GMM	1.00	0.00	1.00	0.25
IBC	0.95	0.85	0.50	0.38
DP	1.00	0.00	1.00	1.00
VQ-BET	1.00	0.00	1.00	0.98

TABLE IV: **Cross-Architecture Transferability Black-Box UAP attack on Lift** : Comparison of average task success rates for unattacked ResNet-18 and ResNet-50 policies. UAP attacks were generated using ResNet-18 BC policies only and deployed on both ResNet-18 and ResNet-50 backbones to assess transferability. Success rates before and after applying UAPs crafted on ResNet-18, revealing generalization of adversarial perturbations across backbone architectures.

Algorithm \ Backbone	ResNet-18		ResNet-50	
	Unattacked	Attacked	Unattacked	Attacked
Vanilla BC	0.72	0.09	0.62	0.20
LSTM-GMM	0.72	0.08	0.56	0.21
IBC	0.74	0.63	0.57	0.27
DP	0.88	0.14	0.78	0.54
VQ-BET	0.62	0.08	0.65	0.29

TABLE V: **Cross-Architecture Transferability Black-Box UAP attack on Push-T** : Comparison of average task success rates for ResNet-18 and ResNet-50 policies. UAP attacks crafted using only ResNet-18 BC policies lead to low task performance on ResNet-50 highlight backbone-level vulnerability.

that Universal Adversarial Perturbation attacks exhibit both cross-algorithm and cross-task transferability, with larger relative performance drops in challenging environments. Moreover, attacks generated with ResNet-18 remain effective on ResNet-50 policies, underscoring that increasing backbone capacity does not eliminate shared vulnerabilities. We believe that our work lays foundation for future work in the direction of adversarial robustness of BC policies. While much progress on adversarial robustness has been made in computer vision, the sequential nature of robotic LfD policies and the complex relationship between vision representations and resulting actions (especially for implicit policies such as IBC and Diffusion Policy) provides an underexplored and

Algorithm	Backbone	ResNet-18		ResNet-50	
		Unattacked	Attacked	Unattacked	Attacked
Vanilla BC		0.75	0.00	0.70	0.34
LSTM-GMM		1.00	0.00	0.25	0.00
IBC		0.09	0.00	0.00	0.00
DP		1.00	0.00	0.875	0.30
VQ-BET		1.00	0.04	0.70	0.70

TABLE VI: **Cross-Architecture Transferability Black-Box UAP attack on Can** : Comparison of average task success rates for ResNet-18 and ResNet-50 policies before and after attack. UAP attacks were crafted solely using ResNet-18 BC policies and directly applied to BC policies trained with ResNet-50 backbone, revealing that adversarial vulnerabilities persist across backbone architectures.

exciting area for future research into both vulnerabilities and defenses.

Our experiments demonstrate that visual perturbations alone are sufficient to degrade performance of modern BC policies, subsequent investigations should extend our analysis to encompass adversarial perturbations applied to other components of the observation space, such as proprioceptive measurements and force sensing. Future work should investigate other types of hybrid state-spaces such as domains with force sensing feedback along with visual feedback to see if visual attacks alone are sufficient to significantly degrade policy performance.

#### REFERENCES

[1] C. Szegedy, W. Zaremba, I. Sutskever, J. Bruna, D. Erhan, I. J. Goodfellow, and R. Fergus, "Intriguing properties of neural networks," *CoRR*, vol. abs/1312.6199, 2013.

[2] I. J. Goodfellow, J. Shlens, and C. Szegedy, "Explaining and harnessing adversarial examples," *CoRR*, vol. abs/1412.6572, 2014.

[3] N. Akhtar and A. Mian, "Threat of adversarial attacks on deep learning in computer vision: A survey," *Ieee Access*, 2018.

[4] W. E. Zhang, Q. Z. Sheng, A. Alhazmi, and C. Li, "Adversarial attacks on deep-learning models in natural language processing: A survey," *ACM Transactions on Intelligent Systems and Technology (TIST)*, vol. 11, no. 3, pp. 1–41, 2020.

[5] A. Chakraborty, M. Alam, V. Dey, A. Chattopadhyay, and D. Mukhopadhyay, "A survey on adversarial attacks and defenses," *CAAI Transactions on Intelligence Technology*, 2021.

[6] G. Hall, A. Das, J. Quarles, and P. Rad, "Studying adversarial attacks on behavioral cloning dynamics," in *2020 IEEE 32nd International Conference on Tools with Artificial Intelligence (ICTAI)*. IEEE, 2020, pp. 452–459.

[7] H. Wu, S. Yunas, S. Rowlands, W. Ruan, and J. Wahlström, "Adversarial driving: Attacking end-to-end autonomous driving," in *2023 IEEE Intelligent Vehicles Symposium (IV)*. IEEE, 2023, pp. 1–7.

[8] A. Boloor, X. He, C. Gill, Y. Vorobeychik, and X. Zhang, "Simple physical adversarial examples against end-to-end autonomous driving models," in *2019 IEEE International Conference on Embedded Software and Systems (ICCESS)*. IEEE, 2019, pp. 1–7.

[9] Y. Chen, H. Xue, and Y. Chen, "Diffusion policy attacker: Crafting adversarial attacks for diffusion-based policies," *ArXiv*, vol. abs/2405.19424, 2024.

[10] A. Mandlekar, D. Xu, J. Wong, S. Nasiriany, C. Wang, R. Kulkarni, L. Fei-Fei, S. Savarese, Y. Zhu, and R. Mart'in-Mart'in, "What matters in learning from offline human demonstrations for robot manipulation," in *Conference on Robot Learning*, 2021.

[11] P. Florence, C. Lynch, A. Zeng, O. Ramirez, A. Wahid, L. Downs, A. Wong, J. Lee, I. Mordatch, and J. Tompson, "Implicit behavioral cloning," *Conference on Robot Learning (CoRL)*, 2021.

[12] C. Chi, S. Feng, Y. Du, Z. Xu, E. Cousineau, B. Burchfiel, and S. Song, "Diffusion policy: Visuomotor policy learning via action diffusion," in *Proceedings of Robotics: Science and Systems (RSS)*, 2023.

[13] S. Lee, Y. Wang, H. Etukuru, H. J. Kim, N. Muhammad, M. Shafiullah, and L. Pinto, "Behavior generation with latent actions," *ArXiv*, vol. abs/2403.03181, 2024.

[14] S.-M. Moosavi-Dezfooli, A. Fawzi, O. Fawzi, and P. Frossard, "Universal adversarial perturbations," *2017 IEEE Conference on Computer Vision and Pattern Recognition (CVPR)*, 2016.

[15] N. Carlini, F. Tramèr, K. D. Dvijotham, L. Rice, M. Sun, and J. Z. Kolter, "(certified!) adversarial robustness for free!" in *The Eleventh International Conference on Learning Representations*. OpenReview, 2023.

[16] Y. Jia, C. M. Poskitt, J. Sun, and S. Chattopadhyay, "Physical adversarial attack on a robotic arm," *IEEE Robotics and Automation Letters*, vol. 7, no. 4, pp. 9334–9341, 2022.

[17] J. Z.-Y. He, D. S. Brown, Z. Erickson, and A. Dragan, "Quantifying assistive robustness via the natural-adversarial frontier," in *Conference on Robot Learning*. PMLR, 2023, pp. 1865–1886.

[18] A. Zhan, S. Tiomkin, and P. Abbeel, "Preventing imitation learning with adversarial policy ensembles," *arXiv preprint arXiv:2002.01059*, 2020.

[19] K. Zhao, H. Huang, M. Li, and Y. Wu, "Rethinking the intermediate features in adversarial attacks: Misleading robotic models via adversarial distillation," *arXiv preprint arXiv:2411.15222*, 2024.

[20] K. Mo, W. Tang, J. Li, and X. Yuan, "Attacking deep reinforcement learning with decoupled adversarial policy," *IEEE Transactions on Dependable and Secure Computing*, vol. 20, pp. 758–768, 2023.

[21] J. Sun, T. Zhang, X. Xie, L. Ma, Y. Zheng, K. Chen, and Y. Liu, "Stealthy and efficient adversarial attacks against deep reinforcement learning," in *AAAI Conference on Artificial Intelligence*, 2020.

[22] A. Pattanaik, Z. Tang, S. Liu, G. Bommanan, and G. V. Chowdhary, "Robust deep reinforcement learning with adversarial attacks," in *Adaptive Agents and Multi-Agent Systems*, 2017.

[23] Y.-C. Lin, Z.-W. Hong, Y.-H. Liao, M.-L. Shih, M.-Y. Liu, and M. Sun, "Tactics of adversarial attack on deep reinforcement learning agents," in *International Joint Conference on Artificial Intelligence*, 2017.

[24] A. Gleave, M. Dennis, N. Kant, C. Wild, S. Levine, and S. J. Russell, "Adversarial policies: Attacking deep reinforcement learning," *ArXiv*, vol. abs/1905.10615, 2019.

[25] H. Zhang, H. Chen, C. Xiao, B. Li, M. Liu, D. Boning, and C.-J. Hsieh, "Robust deep reinforcement learning against adversarial perturbations on state observations," *Advances in Neural Information Processing Systems*, vol. 33, pp. 21 024–21 037, 2020.

[26] H. Zhang, H. Chen, D. Boning, and C.-J. Hsieh, "Robust reinforcement learning on state observations with learned optimal adversary," in *International Conference on Learning Representation (ICLR)*, 2021.

[27] J. Moos, K. Hansel, H. Abdulsamad, S. Stark, D. Clever, and J. Peters, "Robust reinforcement learning: A review of foundations and recent advances," *Machine Learning and Knowledge Extraction*, 2022.

[28] S. Huang, N. Papernot, I. Goodfellow, Y. Duan, and P. Abbeel, "Adversarial attacks on neural network policies," *arXiv preprint arXiv:1702.02284*, 2017.

[29] S. Casper, T. Killian, G. Kreiman, and D. Hadfield-Menell, "White-box adversarial policies in deep reinforcement learning," *arXiv preprint arXiv:2209.02167*, 2022.

[30] X. Chen, W. Guo, G. Tao, X. Zhang, and D. Song, "Bird: generalizable backdoor detection and removal for deep reinforcement learning," *Advances in Neural Information Processing Systems*, 2023.

[31] M. Bain and C. Sammut, "A framework for behavioural cloning," in *Machine Intelligence 15*, 1995, pp. 103–129.

[32] F. Torabi, G. Warnell, and P. Stone, "Behavioral cloning from observation," in *Proceedings of the 27th International Joint Conference on Artificial Intelligence*, 2018, pp. 4950–4957.

[33] S. Ross, G. Gordon, and D. Bagnell, "A reduction of imitation learning and structured prediction to no-regret online learning," in *Proceedings of the fourteenth international conference on artificial intelligence and statistics*, 2011.

[34] S. Hochreiter and J. Schmidhuber, "Long short-term memory," *Neural Computation*, vol. 9, pp. 1735–1780, 1997.

[35] G. J. McLachlan and D. Peel, *Finite mixture models*. John Wiley & Sons, 2000.

[36] J. Ho, A. Jain, and P. Abbeel, "Denosing diffusion probabilistic models," *ArXiv*, vol. abs/2006.11239, 2020.

[37] A. Madry, A. Makelov, L. Schmidt, D. Tsipras, and A. Vladu, "Towards deep learning models resistant to adversarial attacks," in *International Conference on Learning Representations*, 2018.